

Short Communication

Size Effect on Electrochemical Performance of Sodium Terephthalate as Anode Material for Sodium-Ion Batteries

Yi Li[†], Xianfei Hu[†], Haoqing Tang^{*}

School of Chemical Engineering and Technology, Tianjin University, Tianjin 300350, China

[†]These authors contributed equally

^{*}E-mail: liyi-work@qq.com

Received: 22 March 2018 / Accepted: 17 May 2018 / Published: 5 June 2018

Sodium-ion batteries (SIBs) have been recently regarded as one of the most powerful alternatives for lithium ion batteries. Owing to their multi-electron reaction mechanism and low cost, organic anode materials with suitable redox potential and high specific capacity are gradually applied in SIBs. In this article, sodium terephthalate (Na₂C₈H₄O₄, Na₂TP) was synthesized through acid-base neutralization method. Then, Na₂TP with different sizes was obtained by anti-solvent method and applied as anode material for SIBs. The electrochemical performance of Na₂TP improves with its size reducing. When the average size of Na₂TP is 8 μm, the reversible specific capacity reaches 225 mAh/g in the first cycle and remains 166.1 mAh/g after 50 cycles.

Keywords: Sodium-ion batteries; sodium terephthalate; anti-solvent; size adjustment

1. INTRODUCTION

Lithium-ion batteries (LIBs), due to their advantages of high working voltage, large specific capacity, long cycle life, low self-discharge rate and environmental friendliness, have attracted the widespread attention of scientists [1,2]. However, the lithium reserve in the earth's crust is limited, while the current demand for lithium is huge, thus the development of LIBs has gradually entered the bottleneck period [3-5]. Sodium-ion batteries (SIBs), which have similar working principle with LIBs and lower cost, have been taken as the next candidate in energy storage devices [6-8]. In recent years, the research work of cathode materials for SIBs has made great progress. However, the traditional anode material of graphite is not suitable for SIBs [9,10]. Therefore, developing anode material with high energy density and long cycle life, which can match with the cathode materials, are urgently required [11,12].

Owing to their advantages of low cost, favorable safety, environmental friendliness, structural flexibility, and possible multi-electron reactions, organic materials are expected to become the ideal

anode material for SIBs in the future [13,14]. However, there are still some shortcomings: (1) Organic small molecule materials can easily dissolve in organic electrolytes of SIBs according to the principle of “like dissolves like”, resulting in capacity degradation; (2) The conductivity of organic materials is poor, which results in low utilization rate of active materials and large internal resistance of the battery. Researchers are trying to improve the electrochemical performance of organic small molecule materials by preparing corresponding sodium salts, nanosizing, or carbon coating.

Amongst the various organic anode materials, the conjugated carbonyl compounds, which are characterized by even number of conjugated carbonyl functional groups, have been widely studied in LIBs [15]. Conjugated carbonyl compounds mainly include conjugated carboxylates [16], imides [17], quinones [18] with a charge-discharge mechanism of enolization and its reverse reaction. However, at present, there are limited reports of conjugated carbonyl compounds in SIBs. The conjugated carbonyl small molecules sodium salts currently used in SIBs mainly include $\text{Na}_2\text{C}_8\text{H}_4\text{O}_4$ [19,20], $\text{Na}_2\text{C}_6\text{H}_2\text{O}_4$ [18], $\text{Na}_2\text{C}_{12}\text{H}_6\text{O}_4$ [21], $\text{Na}_4\text{C}_8\text{H}_2\text{O}_6$ [22] and so on. Zhao et al. [13] for the first time proposed the application of sodium terephthalate ($\text{Na}_2\text{C}_8\text{H}_4\text{O}_4$, Na_2TP) in SIBs. $\text{Na}_2\text{TP}/\text{KB}$ (Ketjen Black) was synthesized by ball milling method and applied as anode material for SIBs, resulting in good electrochemical performance.

In this paper, we synthesized Na_2TP with different size by anti-solvent method and investigated their electrochemical performance. The conclusion is reached that the electrochemical performance of Na_2TP improves with its size reducing, reaching optimal performance when the average size of Na_2TP is 8 μm . It can be ascribed that smaller Na_2TP size contributes to increasing the contact area between Na_2TP and conductive additive, as well as the electrolyte, thus results in faster migration of Na^+ and improved electrochemical performance.

2. EXPERIMENTAL

2.1. Preparation of pristine Na_2TP

Pristine Na_2TP was prepared by acid-base neutralization method. Sodium hydroxide aqueous solution (40 ml, 1.38 g NaOH, 97%, ACS reagent) was preheated to 60 °C in water bath. 1.73 g of terephthalic acid (99%, AR) powder was added to the above solution under vigorous stirring until it completely dissolved. Then, anhydrous ethanol (98%, AR) was added to the above solution at 90 °C until the solution had just started to precipitate. The above solution was refluxed for 2 hours under 90 °C water bath, and then was filtered. Finally, the precipitation was dried at 80°C for 12 h to obtain pristine Na_2TP powder.

2.2. Size regulation of Na_2TP by anti-solvent method

The size of Na_2TP was adjusted by anti-solvent method. In a typical experiment, we prepared a series of Na_2TP aqueous solutions with different concentration of 30 g/L, 50 g/L, 100 g/L and 150 g/L in water, then added anhydrous ethanol to the above solutions with a volume ratio of 3:1 (ethanol: Na_2TP aqueous solution), respectively. Na_2TP precipitated out from solution with the addition of anhydrous ethanol. The above mixture was filtered to obtain four different sizes of sodium

terephthalate samples, denoted as Na₂TP-30, Na₂TP-50, Na₂TP-100, and Na₂TP-150, respectively.

2.3. Materials characterization

Fourier transform infrared spectroscopy (FTIR) was recorded on a TENSOR II spectrometer (Bruker) with KBr pellets. Powder X-ray diffraction (XRD) pattern was obtained on a DX-27mini desk type X-ray diffractometer (Cu K α radiation) from Dandong Haoyuan Instrument in the range of 10-80°. Scanning electron microscopy (SEM) images were recorded on a Hitachi S-4800 (Japan) scanning electron microscope with a maximum acceleration voltage of 15 kV. Thermogravimetric analysis (TGA, Rigaku, Japan) was performed with a heating rate of 10 °C/min in air.

2.4. Electrochemical measurements

The mixture of active materials, super P and polyvinylidene fluoride (PVDF) was dispersed in N-methyl pyrrolidinone (NMP) at the weight ratio of 65:30:5 to form slurry. All electrodes were prepared by casting the slurry onto copper foil and dried in vacuum at 100 °C for 12 h. The electrochemical performance was examined using 2032 coin-type cells with the as prepared electrode as working electrode, a Na slice as counter electrode, 0.5 M NaCF₃SO₃ (diglyme) as electrolyte, Celgard 2325 as separator. All the cells were assembled in an argon-filled glove box with water and oxygen content both lower than 0.2 ppm and tested at room temperature using a LAND CT2001A battery test system (Wuhan, China) at a potential range of 0.01–1.2 V. Cyclic voltammetry (CV) measurement was performed on a CHI 760E electrochemical workstation (ChenHua Instruments Co., China) under a scan rate of 0.5 mV/s at a potential range of 0.01–1.0 V. Electrochemical impedance spectroscopy (EIS) was recorded by CHI 760E with a frequency range of 0.01-10⁵ Hz. In addition, the specific capacity was calculated based on the mass of Na₂TP.

3. RESULTS AND DISCUSSION

Pristine Na₂TP was characterized by FTIR and XRD, as shown in Figure 1a and b. As depicted in Figure 1a, the peaks located at 1551 cm⁻¹ and 1381 cm⁻¹ indicates the infrared absorption of sodium carboxylate groups (-COONa), which was confirmed by Wan [23]. Figure 1b shows the XRD pattern of pristine Na₂TP, in which all characteristic peaks can be indexed to the space group P2₁/c with JCPDS card NO. 00-052-2146.31 [20], indicating the formation of pristine Na₂TP.

The thermal stability and micromorphology of pristine Na₂TP was characterized by TG and SEM, respectively. As shown in Figure 1c, the TG curve of Na₂TP indicates that Na₂TP remains thermally stable below 500 °C. Therefore, no reactions or phase changes occur corresponding to Na₂TP at room temperature. Figure 1d shows that the pristine Na₂TP distributes inhomogeneously with a size of micrometer scale.

Na₂TP with different sizes was synthesized by anti-solvent method, as depicted in Figure 2. The different color of the bottle depicted in the picture represents the amount of the precipitation. Darker color stands for more precipitation generated.

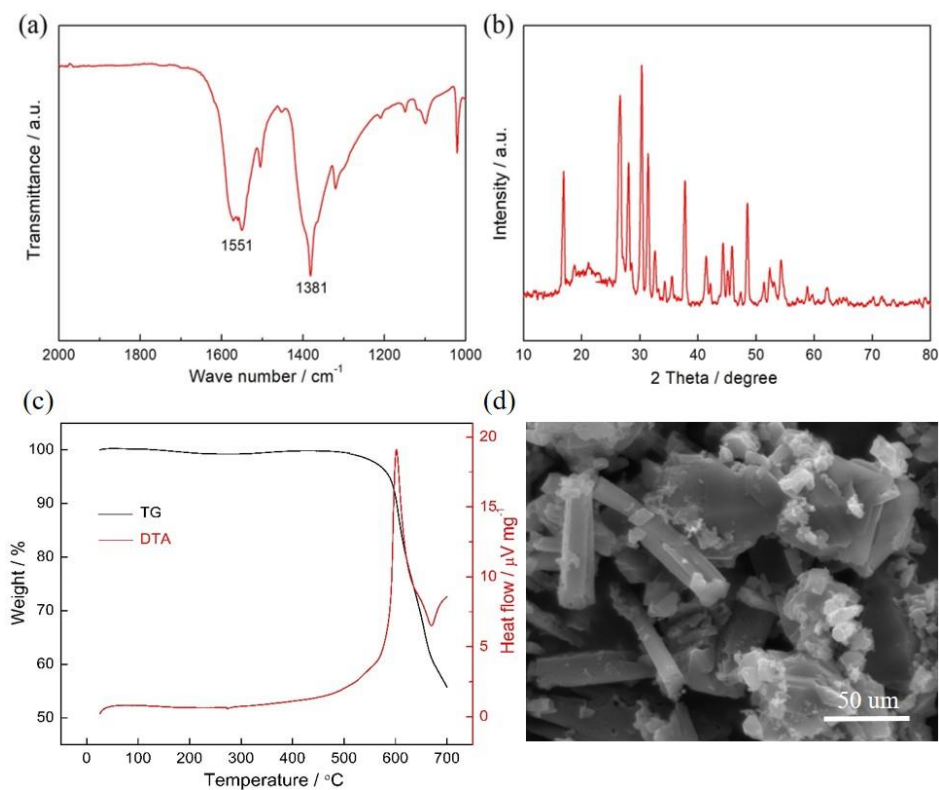


Figure 1. Characterization of pristine Na₂TP: (a) FTIR spectroscopy, (b) XRD pattern, (c) TG curve and (d) SEM image.

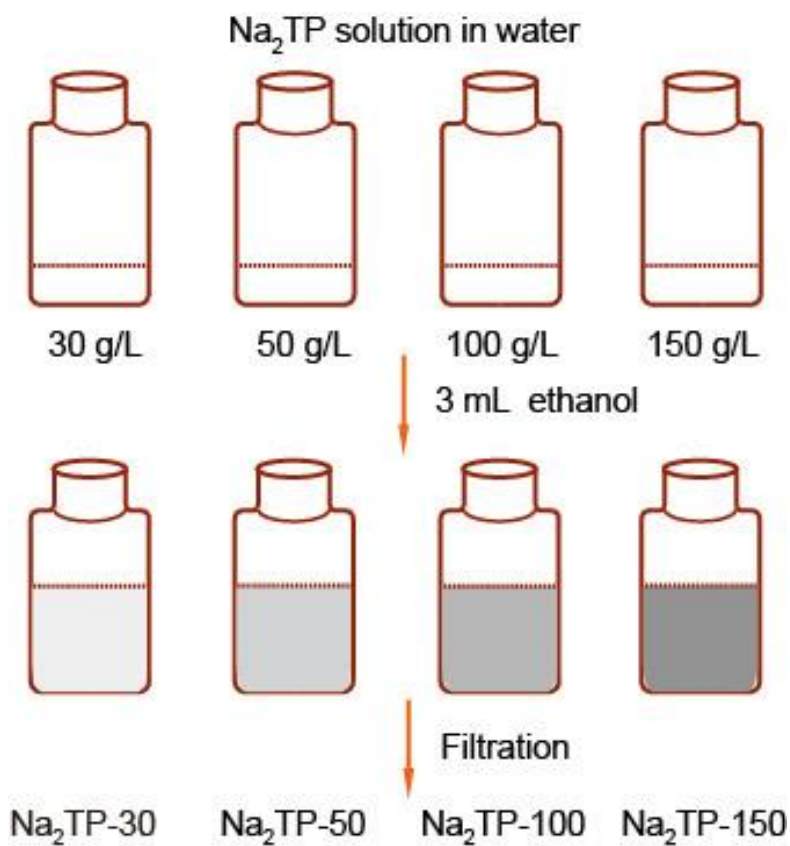


Figure 2. Schematic diagram of preparation process of Na₂TP with different sizes.

Figure 3 shows the morphology of Na_2TP with different sizes, in which the size of Na_2TP reduces with the increasing of the concentration of Na_2TP , while the shape of Na_2TP changes from needle-like shape (Fig. 3a) to particle (Fig. 3g). Compared with pristine Na_2TP , Na_2TP samples prepared by anti-solvent method is much smaller. SEM images of Na_2TP -30 at different magnifications in Fig. 3a and 3b show that Na_2TP -30 has needle-like shape with an average length of 50 μm , and an average diameter of about 6 μm . In comparison, the size of Na_2TP -50 and Na_2TP -100 is much smaller, with a length of about 25 μm and 10 μm , a diameter of about 4 μm and 3 μm , respectively, as shown in Fig. 3c and Fig. 3e. When the concentration of Na_2TP aqueous solution increases to 150 g/L, almost getting the saturation point, the size of corresponding Na_2TP -150 reaches the smallest, with a length of about ~ 8 μm , a diameter of ~ 2 μm .

Owing to its high solubility in water but low solubility in ethanol, Na_2TP precipitates from water with addition of ethanol. In the situation of high concentration of Na_2TP solution, a large amount of Na_2TP nucleation will precipitate from the solution momentarily, without enough time to grow, so the size of Na_2TP -150 is much smaller than that obtained at low concentration of Na_2TP solution.

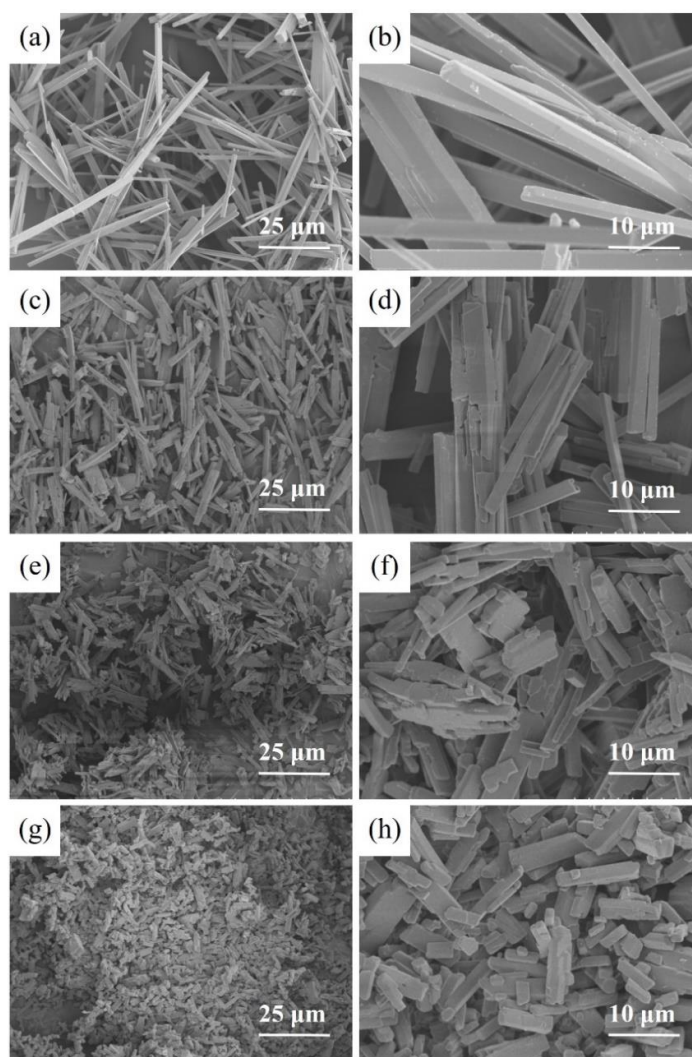


Figure 3. SEM images of Na_2TP -30 (a, b), Na_2TP -50 (c, d), Na_2TP -100 (e, f), and Na_2TP -150 (g, h).

In order to investigate the effect of Na₂TP morphology on its electrochemical performance, the electrochemical performance of as prepared Na₂TP-30, Na₂TP-50, Na₂TP-100 and Na₂TP-150 were tested as anode material in SIBs. The charge-discharge curves and EIS results are shown in Fig. 4a and b. As can be seen from the figure, Na₂TP-150 can deliver an initial reversible capacity of 225 mAh/g at 0.1 C (1 C=255 mA/g), which is very approaching to the theoretical capacity of Na₂TP (255mAh/g) and significantly higher than that of Na₂TP-100 (198 mAh/g), Na₂TP-50 (199 mAh/g) and Na₂TP-30 (202 mAh/g) at the same rate. After 50 charge-discharge cycles, the specific capacity of Na₂TP-30 significantly faded to only 75.9 mAh/g. In comparison, the specific capacity of Na₂TP-50, Na₂TP-100 and Na₂TP-150 faded relatively slowly, remaining 112 mAh/g, 140.9 mAh/g, and 166.1 mAh/g after 50 cycles respectively. Thus the following conclusion was drawn that with the size of Na₂TP reducing, the corresponding specific capacity and cycle stability of Na₂TP improves, which can be ascribed that the contact area of Na₂TP with conductive additive and electrolyte increases with the size reduction of Na₂TP, resulting in the smaller size of Na₂TP and faster migration of sodium ions in Na₂TP.

EIS measurement was conducted to compare the electrochemical impedance of Na₂TP with different sizes, as shown in Fig 4b. The part of semicircle in EIS curve represents electrochemical reaction impedance (R_{ct}), while the linear part represents the Warburg impedance (R_w). It can be seen that the electrochemical impedance decreases with the reduction of the size of Na₂TP, while Na₂TP-150 possesses the lowest resistance, which is consistent with the results in Fig.4a.

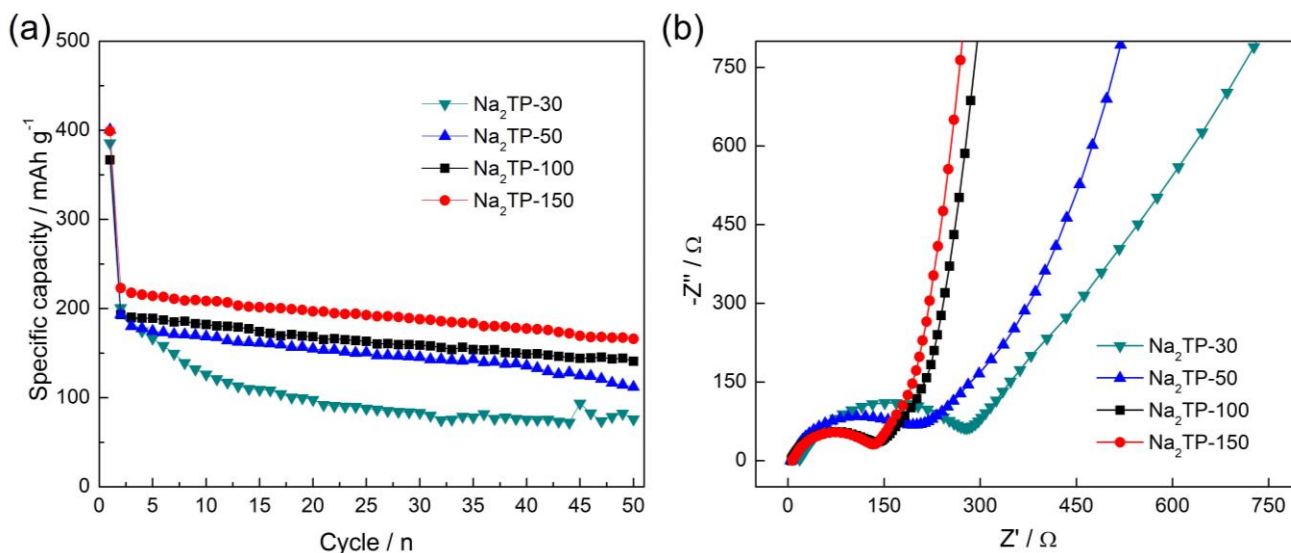


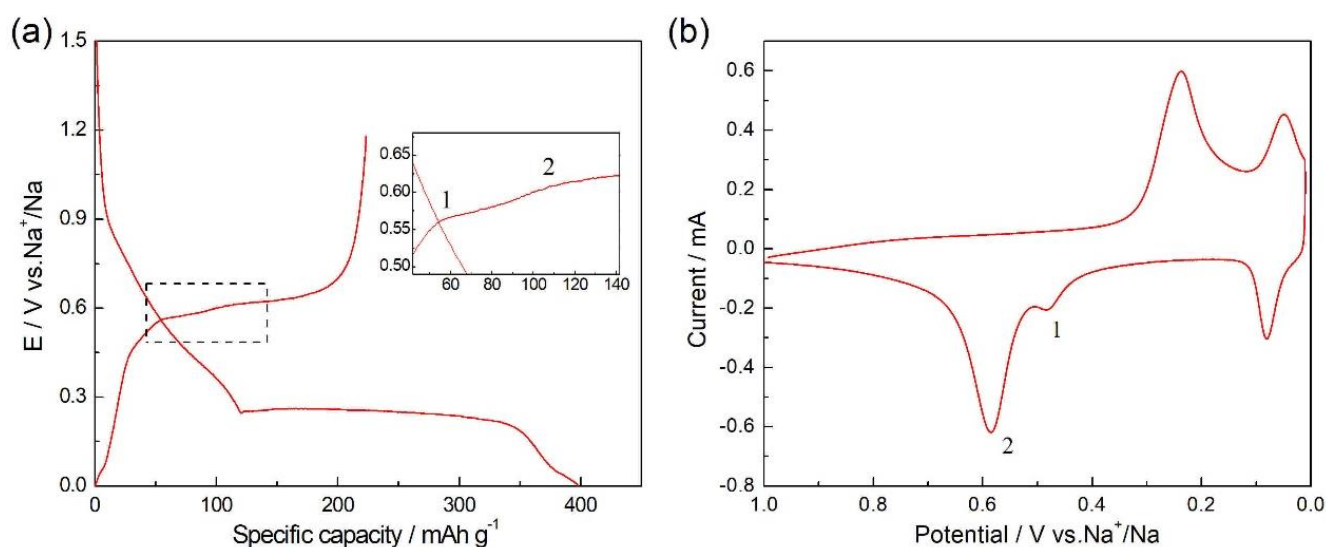
Figure 4. (a) Cyclic performance at 0.1 C and (b) EIS plots of Na₂TP with different sizes as the anode materials of SIBs.

Table 1 depicts the electrochemical performance of Na₂TP reported in other articles, in which the current density, initial reversible capacity, initial Coulombic efficiency and active material content are listed. Through this comparison, we can find that Na₂TP-150 in this article stands out for its modest initial reversible capacity (225 mAh/g), high initial Coulombic efficiency (56.3%) at 0.1 C (25.5 mA/g) and high active material content (65%) without any complicated modification process.

Table 1. Comparison of electrochemical performance of Na₂TP

Sample	Cycling performance				Ref
	Current density	Initial reversible capacity (mAh g ⁻¹)	Initial Coulombic efficiency	Active material content (wt. %)	
Na ₂ TP@GE	100 mA/g	270	27.6%	66%	[20]
NS-Na ₂ TP	250 mA/g	248	34.3%	40%	[23]
Na ₂ TP/KB	0.1 C	250	50.3%	64%	[13]
ALD-20	0.1 C	275	60.5%	64%	[13]
Na ₂ TP/KB	0.1 C	225	56.3%	65%	This work

In addition, we tested the first cycle of charge-discharge curve and CV curve to investigate the reaction mechanism of Na₂TP using Na₂TP-150 as work electrode. As shown in Fig.5a, the discharge platform located at 0.04 V and the charge platform located at 0.1 V can be ascribe to the reversible insertion or extraction process of Na⁺ in super P, which was consistent with the report in Wan [23] and Choi [16]. We can also confirm this point according to the pair of reversible redox peaks located at 0.1/0.04 V (vs. Na⁺/Na) in CV curve (Fig. 5b). The platform located at 0.3 V (vs. Na⁺/Na) during the discharging process, indicates a single step process of two-electron reaction of reversible insertion or extraction process of Na⁺ in Na₂TP [24]. However, during the following charging process, two voltage plateaus located at 0.40 V and 0.60 V (vs. Na⁺/Na) can be observed in Fig 5a, indicating a two-step process of two-electron reaction of reversible insertion or extraction process of Na⁺ in Na₂TP, which is in accord with the anodic peaks (0.49 and 0.59 V vs. Na⁺/Na) in CV profile.

**Figure 5.** (a) The first cycle of charge-discharge curve at 0.1 C and (b) the CV curve at a scan rate of 0.5 mV/s of Na₂TP-150.

4. CONCLUSIONS

In this study, pristine Na₂TP was prepared by acid-base neutralization method. Then, through anti-solvent method, four different sizes of Na₂TP, which can be denoted as Na₂TP-30, Na₂TP-50,

Na₂TP-100 and Na₂TP-150, was obtained. Electrochemical characterization shows that with an average size of 8 μm, the initial reversible specific capacity of Na₂TP-150 is about 225 mAh/g at a rate of 0.1 C. After 50 cycles, the specific capacity remains at 166.1 mAh/g. The size reduction of Na₂TP increases its contact area with conductive additives and electrolytes, thus resulting in high migration rate of Na⁺ and excellent electrochemical performance of Na₂TP as anode material for SIBs.

References

1. J. B. Goodenough, K. S. Park, *J. Am. Chem. Soc.*, 135 (2013) 1167.
2. J. M. Tarascon, *Nat. Chem.*, 2 (2010) 510.
3. J. M. Tarascon, M. Armand, *Nature*, 414 (2001) 359.
4. M. D. Slater, D. Kim, E. Lee, C. S. Johnson, *Adv. Funct. Mater.*, 23 (2013) 947.
5. B. L. Ellis, L. F. Nazar, *Curr. Opin. Solid St. M.*, 16 (2012) 168.
6. Z. Yang, J. Zhang, M. C. Kintner-Meyer, X. Lu, D. Choi, J. P. Lemmon, J. Liu, *Chem. Rev.*, 111 (2011) 3577.
7. S.-W. Kim, D.-H. Seo, X. Ma, G. Ceder, K. Kang, *Adv. Energy Mater.*, 2 (2012) 710.
8. S. P. Ong, V. L. Chevrier, G. Hautier, A. Jain, C. Moore, S. Kim, X. Ma, G. Ceder, *Energ. Environ. Sci.*, 4 (2011) 3680.
9. J. Sangster, *J. Phase Equilib. Diffus.*, 28 (2007) 571.
10. K. Nobuhara, H. Nakayama, M. Nose, S. Nakanishi, H. Iba, *J. Power Sources*, 243 (2013) 585.
11. V. Palomares, P. Serras, I. Villaluenga, K. B. Hueso, J. Carretero González, T. Rojo, *Energ. Environ. Sci.*, 5 (2012) 5884.
12. H. Pan, Y.-S. Hu, L. Chen, *Energ. Environ. Sci.*, 6 (2013) 2338.
13. L. Zhao, J. Zhao, Y.-S. Hu, H. Li, Z. Zhou, M. Armand, L. Chen, *Adv. Energy Mater.*, 2 (2012) 962.
14. Y. Park, D. S. Shin, S. H. Woo, N. S. Choi, K. H. Shin, S. M. Oh, K. T. Lee, S. Y. Hong, *Adv. Mater.*, 24 (2012) 3562.
15. M. Armand, S. Grugeon, H. Vezin, S. Laruelle, P. Ribiere, P. Poizot, J. M. Tarascon, *Nat. Mater.*, 8 (2009) 120
16. A. Choi, Y. K. Kim, T. K. Kim, M.-S. Kwon, K. T. Lee, H. R. Moon, *J. Mater. Chem. A.*, 2 (2014) 14986.
17. H. Banda, D. Damien, K. Nagarajan, M. Hariharan, M. M. Shaijumon, *J. Mater. Chem. A.*, 3 (2015) 10453.
18. Z. Zhu, H. Li, J. Liang, Z. Tao, J. Chen, *Chemical communications*, 51 (2015) 1446.
19. M. A. Sk, S. Manzhos, *J. Power Sources*, 324 (2016) 572.
20. Y. Wang, K. Kretschmer, J. Zhang, A. K. Mondal, X. Guo, G. Wang, *RSC Adv.*, 6 (2016) 57098.
21. W. Deng, J. Qian, Y. Cao, X. Ai, H. Yang, *Small*, 12 (2016) 583.
22. X. Wu, J. Ma, Q. Ma, S. Xu, Y.-S. Hu, Y. Sun, H. Li, L. Chen, X. Huang, *J. Mater. Chem. A.*, 3 (2015) 13193.
23. F. Wan, X.-L. Wu, J.-Z. Guo, J.-Y. Li, J.-P. Zhang, L. Niu, R.-S. Wang, *Nano Energy*, 13 (2015) 450.
24. C. Wang, Y. Xu, Y. Fang, M. Zhou, L. Liang, S. Singh, H. Zhao, A. Schober, Y. Lei, *J. Am. Chem. Soc.*, 137 (2015) 3124.